# Method and some results of numerical simulation of the intensity fluctuations of a plane light wave behind a phase screen in a multipath region. Part 2. Fluctuations behind a one-dimensional screen

**V.V. Vorob'ev**

*A.M. Obukhov Institute of Atmospheric Physics, Russian Academy of Sciences, Moscow*

Received October 22, 2001

The relations between the distribution of the refraction angle fluctuations over statistically nonuniform phase screen and fluctuations of light intensity averaged over the receiver's aperture in the multipath area are obtained. The conditions of applicability of these relations are analyzed. Based on these conditions, numerical simulation of stellar scintillations observed through the Earth's atmosphere from space is carried out. A good agreement is obtained between the statistical characteristics of simulated and actual stellar scintillations.

In the first part of this paper,[1] equations have been derived for calculation of scintillation characteristics averaged over an ensemble of realizations and over the receiver's aperture, and conditions have been formulated for their applicability. In this part, I present some results of numerical simulation of scintillations caused by stratified atmospheric inhomogeneities, which can be modeled by a one-dimensional phase screen.

Define the mean intensity as an average over a rectangular receiving aperture with the halfwidths $R_z$ along the vertical axis and $R_y$ along the horizontal axis

$$I_S(z,R_z,R_y)=\frac{1}{4R_zR_y}\int\limits_{-R_z}^{R_z}\int\limits_{-R_y}^{R_y}I(z+z',y+y')\mathrm{d}z'\mathrm{d}y'. \quad (1)$$

Unlike similar definition in Ref. 1, there is no averaging over realizations here and $I_S$ is a fluctuating characteristic.

From analysis in Ref. 1 it follows that in the case that the aperture dimensions $R_z$ and $R_y$ are much larger than the characteristic spatial dimensions of the near-caustic zone $l_k$ the average intensity of light behind the phase screen, a plane wave of the unit intensity is incident on, can be calculated as

$$I_S(z,y)=\frac{1}{4R_zR_y}\int\limits_{-\infty}^{\infty}\int\limits_{-\infty}^{\infty}\theta\left[1-\left(\frac{\eta+L\gamma_\eta(\eta,\zeta)-z}{R_z}\right)^2\right]\times$$

$$\times\theta\left[1-\left(\frac{\zeta+L\gamma_\zeta(\eta,\zeta)-y}{R_y}\right)^2\right]\mathrm{d}\zeta\,\mathrm{d}\eta, \quad (2)$$

where $\eta$ and $\zeta$ are the coordinates of points on the phase screen; $\theta(x)$ is the unit stepwise function; $\gamma_\eta(\eta,\zeta)=\partial S(\eta,\zeta)/\partial\eta$, $\gamma_\zeta(\eta,\zeta)=\partial S(\eta,\zeta)/\partial\zeta$ are the components of the refraction angles; $S(\eta,\zeta)$ is the eikonal distribution over the phase screen; $L$ is the distance from the screen to the observation plane.

In this paper, we consider the case of a one-dimensional phase screen, the distribution of the refraction angle over which is specified as a function of one variable $\eta$: $\gamma(\eta)=\gamma_\eta(\eta)=\partial S(\eta)/\partial\eta$. With the wish to apply the results to interpretation of scintillation measurements from space, let us choose the coordinate axis as a vertical passing through the perigee point of the light beam mean for the measurement range with coordinates measured from the Earth's surface. In this case $\gamma_\zeta=0$ and $l_k$ is determined as follows:

$$l_k(\eta)=\frac{L}{k}\left(k\frac{27}{24}\frac{\mathrm{d}^3S(\eta)}{\mathrm{d}\eta^3}\right)^{1/3},$$

and Eq. (2), after integration over the coordinate $\zeta$, takes the form

$$I_S(z)=\frac{1}{2R_z}\int\limits_{-\infty}^{\infty}\theta\left[1-\left(\frac{\eta+L\gamma(\eta)-z}{R_z}\right)^2\right]\mathrm{d}\eta. \quad (3)$$

The conditions for applicability of the equation similar to Eq. (3) were found in Ref. 1 based on the estimated differences of the integrand function from the stepwise $\vartheta$-function with the allowance made for cubic term in the series expansion of the eikonal difference at two points. To illustrate the efficiency of this equation, here we present a comparison of the exact and approximate solutions of the problem of light diffraction behind a Gaussian phase screen with the distribution $\varphi(z)=kS(z)=-30\pi\exp[-(z/l_0)^2]$ and $l_0=5$ m at $L=3000$ km. The wavenumber $k$ in calculations is taken to be equal to $10^7\ \mathrm{m}^{-1}$. A screen with such

0235-6880/02/07 510-05 $02.00 

parameters makes a complex diffraction pattern in the observation plane. The central part of this pattern is shown in Fig. 1*a*. It was calculated by use of fast Fourier transform method.

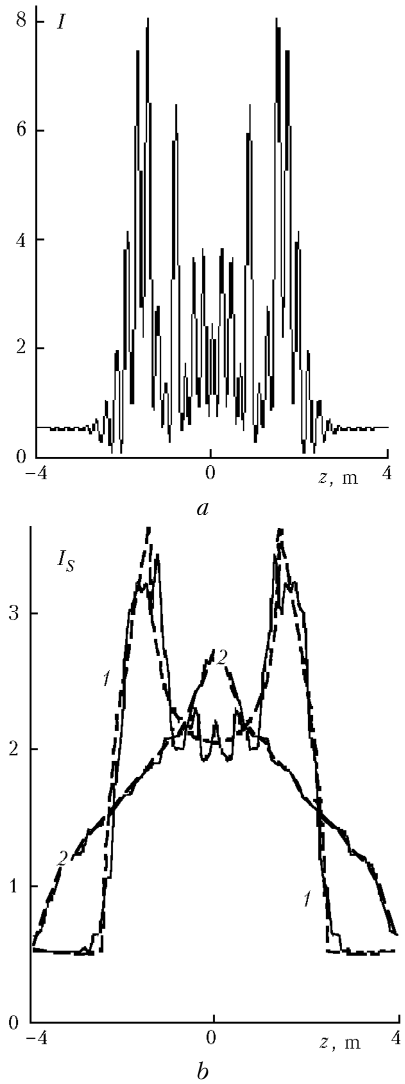


**Fig. 1.** Intensity distribution in the multipath region at diffraction of a plane wave on a screen with a Gaussian phase perturbation. Non-averaged distribution (*a*), averaged distribution (*b*) at the aperture halfwidth of 0.5 (*1*) and 2 m (*2*); the exact solution (solid curves) and approximate solution (dashed curves).

Figure 1*b* shows the distributions of the average intensities calculated by a moving average over the apertures with the halfwidths of 0.5 and 2 m. The solid curves in Fig. 1*b* show the results of averaging of the exact intensity distributions, and dashed ones are the intensity distributions calculated by Eq. (3). The maximum value of the scale $l_k(z)$ at the given distance $L$ and phase screen parameters is equal to 0.45 m. It can be seen from Fig. 1 that already at $R_z$ = 0.5 m the difference between the approximate and exact dependences is small, and at $R_z$ = 2 m the approximate and exact dependences coincide within the accuracy of the graphical presentation. In this particular example this means that the condition $R_z > 4\ l_k$ must be fulfilled accurate to about 2%.

This example shows that Eq. (3) is applicable to calculations in the case that the size of inhomogeneities is relatively small, about several meters for the geometry of observations from orbiting stations, if the dimensions of the effective averaging aperture are smaller than several meters. This allows simple modeling of scintillations behind the atmosphere with large-scale stratified inhomogeneities arising at internal wave fall.[2,3] The minimum scales of such inhomogeneities do not exceed 10 m. Some results of statistical modeling of scintillations behind a one-dimensional phase screen are given below.

As is seen from Eq. (2), the distribution of the aperture-averaged intensity of the light field behind the phase screen is independent of the wavenumber being completely determined by the distribution of the refraction angle on the screen.

In this paper, Eq. (3) was used to calculate the average intensity behind the phase screen with the refraction angle distribution $\gamma(z)$ of the following form:

$$\gamma(z) = \gamma_0(z)\ [1 + d\gamma\ g(z)], \tag{4}$$

where $\gamma_0(z)$ is the mean height distribution of the refraction angle; $d\gamma$ is the square root of the variance of relative fluctuations of the refraction angle; $g(z)$ is the function having normal distribution, zero mean, and unit variance. The spatial spectrum of this function was specified in the following form:

$$Fg(p) = \frac{C}{1+(pL_0)^2} \exp[-(pl_0)^2]\,, \tag{5}$$

where the coefficient $C$ was chosen from the normalization

$$\langle g^2 \rangle = \int_{-\infty}^{\infty} Fg(p)\mathrm{d}p = 1\,. \tag{6}$$

The inertial part of the spectrum (5) corresponds to the spectrum of eikonal fluctuations on the screen $F_S(p) \sim 1/p^4$, that is characteristic of turbulence caused by the internal wave fall.[2] The value of $d\gamma$ in calculations was taken equal to 0.02, and the internal $l_0$ and external $L_0$ scales of turbulence were taken equal to 50 and 1000 m. Realizations of the distribution of the refraction angle were modeled by the method of white noise filtration.[4]

The exponential distribution

$$\gamma_0(z) = \gamma(z_0) \exp\left(\frac{z_0 - z}{H_0}\right)$$

with $z_0 = 30$ km, $H_0 = 6.25$ km, and $S_0 = L\gamma(z_0) =$ $= 1.124$ km was taken as the mean one.

To take into account the effect of extinction of light due to molecular scattering, which is important for interpretation of actual observations, intensity realizations calculated by Eq. (3) as functions of height of the ray perigee $\eta$ at the heights lower than $\eta_1$ = 40 km were multiplied by the transmission function

$$F_{\rm ext}(\eta) = \exp[A_1 (\eta - \eta_1) - A_2 (\eta - \eta_1)^2 + + A_3 (\eta - \eta_1)^3]$$

with the parameters $A_1 = 0.02$, $A_2 = 0.0003$, and $A_3 = 0.00008$.

Figure 2 exemplifies realization of the scintillation intensity $I_S$ at the receiver with the aperture halfwidth $R_z$ = 2 m as a function of the perigee height, as well as 0.5-km long parts of this realization at different perigee heights.

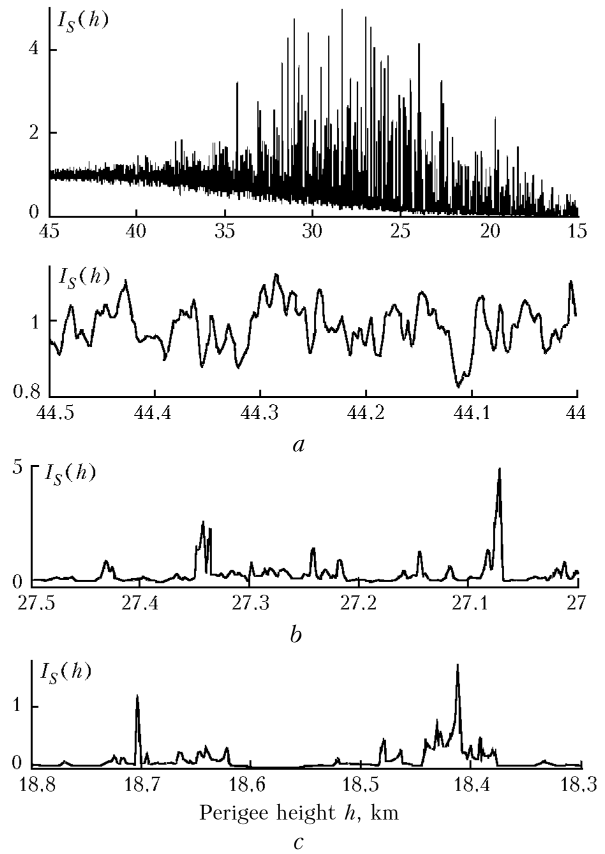

**Fig. 2.** Simulated realization of the scintillation intensity $I_S$ and its fragments in the regions of weak fluctuations (*a*), focusing (*b*), and multipathing (*c*).

If we compare the simulated scintillations with the measured ones, that is, Fig. 2 of this paper with Fig. 3 of Ref. 2 and Fig. 2 with Figs. 4 and 5 of Ref. 3, then we can see a good qualitative and quantitative agreement. Thus, in the focusing region (at the ray perigee heights of about 29 km in the field experiment and about 27 km in the numerical one), a characteristic pattern is the presence of spikes about 10 to 20-m wide separated roughly by 300 to 400 m. The multipath zone is characterized by the signal fadeaway down to a series of pulses separated by deep fade intervals. The effective width of the pulses increases, as the ray perigee height decreases. The difference between the actual and simulated realizations consists in the fact that in the actual ones there is high-frequency modulation of multiplicative noise. This modulation is likely caused by the effect of small-scale Kolmogorov turbulence, which is ignored in numerical simulations.

Equations (2) and, especially, (3) allow one to easily conduct statistical simulation and studying the properties of strong fluctuations in both statistically homogeneous and inhomogeneous media based, as well as checking theoretical conclusions drawn from application of different asymptotic methods.

Below we consider, as a case study, the issue of applicability of perturbation methods to calculation of the variance of intensity fluctuations averaged over the aperture.

In Ref. 5 it was shown, in particular, that to calculate the low-frequency part of the scintillation spectrum behind a statistically uniform, single-scale random screen, equations of the method of smooth perturbations (MSP) are applicable. According to asymptotic estimates,[5] these equations must be fulfilled for the spectrum at the wavenumbers

$$q < q_1 = \sqrt{\frac{l^2}{2 < dS^2 > L^2}}\,, \tag{7}$$

where $l$ is the scale of phase screen inhomogeneities; $<dS^2>$ is the variance of eikonal fluctuations on the screen. At the distribution (4), $<dS^2>/l^2 \approx [\gamma_0(z)\, d\gamma]^2$ and the wavenumber

$$q_1(\eta) = \frac{1}{\sqrt{2}R_1} \approx \frac{1}{\sqrt{2}L\gamma_0(\eta)d\gamma}\,. \tag{8}$$

The characteristic $R_1$ inverse to $q_1$ is equal, by the order of magnitude, to the square root of the variance of ray displacements in the observation plane. The intensity fluctuations averaged over the aperture are determined by the spectral components with $q \le R_z^{-1}$, therefore it can be expected that the MSP equations (in the region of strong not averaged fluctuations) can be fulfilled not only in the low-frequency part of the spectrum, but also for the variance of intensity fluctuations if $q_1 R_z > C_1$. Here $C_1$ is on the order of unity. Numerical experiment allows one to refine the applicability of this assumption.

Figure 3 depicts the calculated results on the height dependence of the variance of average intensity fluctuations calculated using 200 realizations obtained at the same values of the phase screen parameters as those, at which one of the realizations shown in Fig. 2 was simulated. In this case $R_1$ is about 30 m at the ray perigee height of 30 km. The variance of intensity fluctuations $\beta_0(\eta)$ as calculated by equations of the first approximation of the perturbation method is shown as well.

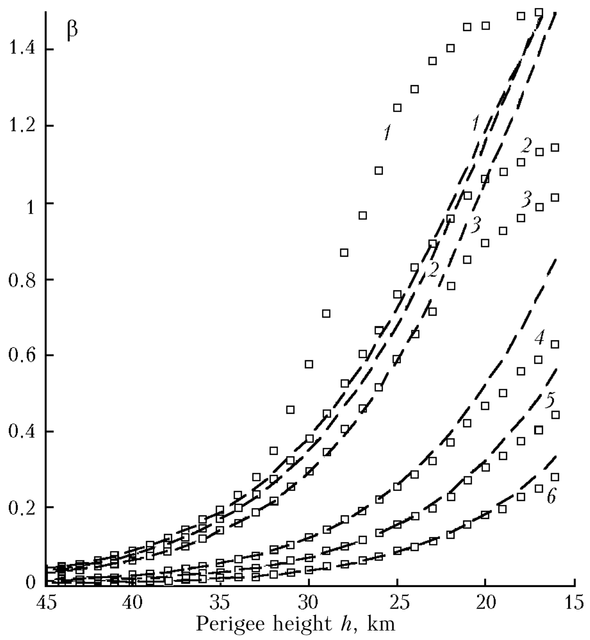


**Fig. 3.** Index of average scintillations β as a function of the ray perigee height at the halfwidth of the averaging aperture equal to 1 (*1*), 10 (*2*), 20 (*3*), 100 (*4*), 200 (*5*), and 400 m (*6*); results of numerical simulation of strong scintillations with the following averaging (squares), calculation by equations of the perturbation method (dashed lines).

These equations were derived in the following way. Let us write the height dependence of the refraction angle in the following form:

$$\gamma(\eta) = \gamma_0(\eta) + \gamma_1(\eta),$$

where $\gamma_1(\eta) = \gamma_0(\eta)\ d\gamma\ g(\eta)$ is the fluctuating part.

Assume that in the absence of fluctuations light propagates in the single-path mode and fluctuations of the refraction angle are small ($|\gamma_1(\eta)| \ll |\gamma_0(\eta)|$). Let $\eta_0$, $\eta_1$, and $\eta_2$ be the roots of the equations:

$$\eta_0 + L\gamma_0(\eta_0) = z,\ \eta_1 + L\gamma(\eta_1) = z - R_z,$$

$$\eta_2 + L\gamma(\eta_2) = z + R_z.$$

If the fluctuations $\gamma_1$ are small, the solutions of the last two equations are as follows:

$$\eta_1 = \eta_0 - QR_z\left[1 + \frac{L}{R_z}\gamma_1(\eta_0 - QR_z)\right],$$

$$\eta_2 = \eta_0 + QR_z\left[1 - \frac{L}{R_z}\gamma_1(\eta_0 + QR_z)\right],$$

where

$$Q(z) = Q\ [\eta_0(z)] = [1 + L\mathrm{d}\gamma_0(\eta_0)/\mathrm{d}\eta_0]^{-1}$$

is the coefficient of the refraction weakening.

For the aperture-average intensity and its relative fluctuations we have, from Eq. (3), the following equations:

$$I_S(z) = I_S[\eta_0(z)] = \frac{\eta_2(z) - \eta_1(z)}{2R_z} =$$

$$= Q(z)\left(1 + \frac{L}{R_z}[\gamma_1(\eta_0 - QR_z) - \gamma_1(\eta_0 + QR_z)]\right),$$

$$I_1(\eta) = I_S(\eta)/Q(\eta) - 1 =$$

$$= \frac{L}{R_z}[\gamma_1(\eta_0 - QR_z) - \gamma_1(\eta_0 + QR_z)]. \qquad (9)$$

Having assumed that the spatial scale of the fluctuating part of the refraction angle is much smaller than the spatial scale of the regular part, the following equation follows from Eq. (9) for the squared variance of the relative intensity fluctuations:

$$\beta_0^2(\eta) = \langle I_1^2(\eta)\rangle = \frac{4L^2}{R_z^2}[\gamma_0(\eta)d\gamma]^2 \times$$

$$\times \int_{-\infty}^{\infty} Fg(p)\sin^2[R_zQ(\eta)p]\,\mathrm{d}p. \qquad (10)$$

From the data shown in Fig. 3, it can be concluded that, actually, to calculate the variance of intensity fluctuations with averaging over a large aperture in both the focusing and random multipathing regions, equations of the first approximation of the perturbation method (corresponding to the equations of the method of smooth perturbations for field calculation) can be applied.

If the average intensity fluctuations are weak so that Eq. (10) is applicable to their calculation, then at the normal distribution of refraction angle fluctuations they also must obey normal distribution. The validity of this statement was checked using a statistically uniform screen as an example. (In the case of statistically nonuniform screen, it is difficult to conduct such a simulation because of the need to simulate a large number of realizations for statistically confident conclusions.)

Figure 4 depicts the calculated probability density of the average intensity distribution in the case of small, as compared with $R_1$, and large averaging apertures. Four hundreds of screen realizations with the parameters $\gamma_0(\eta) =$ = const, $R_1 = L\gamma_0\,d\gamma = 100$ m, and the spectrum (5) with $l_0 = 50$ m and $L_0 = 500$ m were simulated. Crosses in Fig. 4 stand for the results of numerical simulation at the aperture halfwidth $R_z = 0.5$ m, and circles are for those at $R_z = 200$ m. The variances of average fluctuations were $\beta_1 = 1.25$ at $R_z = 0.5$ m and $\beta_2 = 0.256$ at $R_z = 200$ m.

It can be seen from Fig. 4 that at large averaging aperture the probability distribution of average intensity fluctuations is more similar to the normal than to the lognormal one. At small averaging apertures, the probability distribution at $I_S \geq 0.7$ is similar to the lognormal one, and if $I_S < 0.7$ it differs significantly from the lognormal distribution and even more from the normal one. These results mostly agree with the results of analysis of scintillations in the actual experiment.[3] There is some difference in the probability distributions of high spikes and deep fades. Their probability in the actual experiment was higher than that in the numerical one. This difference is likely caused by the presence of instrumental noise in measurements that is significant in the fade zone and by the lack of statistical confidence in high spikes. It should be noted that in the numerical experiment, as model ones, the parameters ($R_1$, $l_0$, $L_0$, $d\gamma$) were varied in wide limits and we observed no probability distributions close to the exponential distribution, which is widely used for calculation of fluctuation characteristics in the saturation zone. It was already noticed earlier that the exponential distribution was not observed in field measurements as well.[6]

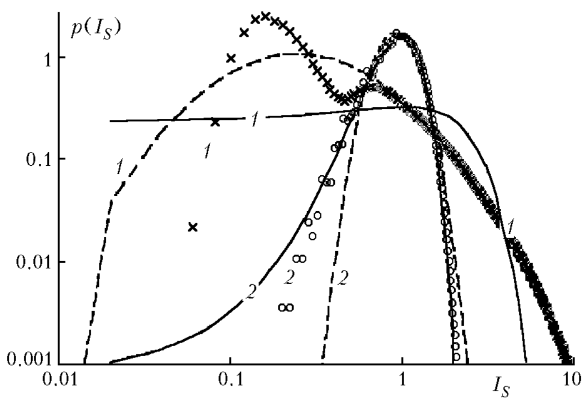


**Fig. 4.** Probability density distribution $p(I_S)$ of the intensity fluctuations of light averaged over the receiver aperture in the multipath region behind a statistically uniform screen at the averaging amplitude halfwidth $R_z$ = 0.5 (*1*) and 200 m (*2*); numerical experiment (crosses and circles), lognormal distribution (dashed line), and normal distribution with the parameters $\beta_1$ and $\beta_2$ (solid line).

The investigations carried out have proven the applicability of equations of the perturbation method to calculation of the characteristics of scintillations measured with a large-aperture receiver. This conclusion may turn out useful for practical applications when developing methods for description of scintillations and in spectroscopic methods of determination of gaseous constituents of the atmosphere from measurements of stellar radiation from space platforms.[7] The characteristic size of the averaging aperture in this case is the height interval, the receiver travels during the time between successive measurements. At the measurement rate equal to several hertzs, depending on the orbit position relative to the direction toward the star, the averaging interval can be from 100 to 1000 m.

However, it should be kept in mind that Eq. (10) was obtained assuming the regular wave structure (in the absence of fluctuations) to be single-path in the observations plane. In the models of regular refraction allowing for multipathing mode, as was shown in Ref. 1, even the average height distribution of the light intensity may have a complex structure. The issue of applicability of the perturbation method to calculation of the characteristics of fluctuations calls for a separate consideration.

## Conclusions

Simple equations have been obtained that relate the distribution of refraction angle fluctuations over a nonuniform phase screen to the distribution of the light intensity averaged over the receiver aperture in the multipath region. Based on these equations, numerical simulation of the process of stellar scintillation at observation through the Earth's atmosphere from space has been carried out.

Using the model of exponential regular atmosphere as a case study, the dependence of the variance of average scintillations on the perigee height of a light ray and on the size of the averaging aperture has been studied. The probability distributions of the intensity of scintillations have been calculated.

It has been confirmed that the large-scale portion of the spectrum of strong fluctuations is described by the equations of the perturbation method. It has been noticed that in the region of strong fluctuations the statistics of intensity spikes is close to the lognormal one. Numerical simulation has demonstrated the invalidity of the assumption widely used in the asymptotic theory that if fluctuations are close to saturation, then their distribution is close to the exponential one.

### Acknowledgments

The author is thankful to A.S. Gurvich and V. Kan for manuscripts of Refs. 2 and 3 and discussion of the results.

This work was partly supported by the Russian Foundation for Basic Research (Projects No. 01–02–16213 and No. 01–05–64944).

### References

1. V.V. Vorob'ev, Atmos. Oceanic Opt. **15**, No. 7, 505–509 (2002).
2. A.S. Gurvich, V. Kan, S.A. Savchenko, A.I. Pakhomov, P.A. Borovikhin, O.N. Volkov, A.Yu. Kaleri, S.V. Avdeev, V.G. Korzun, G.I. Padalka, and Ya.P. Podvyaznyi, Izv. Ros. Akad. Nauk, Ser. Fiz. Atmos. Okeana **37**, No. 4, 469–486 (2001).
3. A.S. Gurvich, V. Kan, S.A. Savchenko, A.I. Pakhomov, and G.I. Padalka, Izv. Ros. Akad. Nauk, Ser. Fiz. Atmos. Okeana **37**, No. 4, 487–501 (2001).
4. J.A. Fleck, J.R. Morris, and M.D. Feit, Appl. Phys. **10**, No. 1, 129–160 (1976).
5. V.I. Shishov, Izv. Vyssh. Uchebn. Zaved., Ser. Radiofizika **14**, No. 1, 85–92 (1971).
6. A.S. Gurvich, A.I. Kon, V.L. Mironov, and S.S. Khmelevtsov, *Laser Radiation in the Turbulent Atmosphere* (Nauka, Moscow, 1976), 277 pp.
7. A.V. Polyakov, Yu.M. Timofeev, A.S. Gurvich, V.V. Vorob'ev, and V. Kan, Izv. Ros. Akad. Nauk, Ser. Fiz. Atmos. Okeana **37**, No. 1, 56–66 (2001).